Available online at www.sciencedirect.com

SciVerse ScienceDirect

journal homepage: www.elsevier.com/locate/he

Experimental analysis of a PEM fuel cell performance at variable load with anodic exhaust management optimization

B. Belvedere [a], M. Bianchi [a], A. Borghetti [a], A. De Pascale [a,*], M. Paolone [b], R. Vecci [a]

[a] Faculty of Engineering, University of Bologna, Viale del Risorgimento 2, 40136 Bologna, Italy
[b] Distributed Electrical Systems Laboratory, EPFL, 1015 Lausanne, Switzerland

ARTICLE INFO

Article history:
Received 16 March 2012
Received in revised form
22 September 2012
Accepted 24 September 2012
Available online 18 October 2012

Keywords:
Fuel cell
PEM
Flooding
Purge process
Outlet purge valve

ABSTRACT

In this paper an investigation on the performance of a commercial Proton Exchange Membrane (PEM) fuel cell, installed at the laboratory of the University of Bologna, is carried out, taking into account the anodic exhaust management and its effects on the flooding phenomenon.

To address the problem of flooding, it is necessary to run periodically the purge process of the Fuel Fell (FC). Indeed, in this study the periodic anodic purge process in dead-end mode has been investigated. This operation is performed by opening a particular control valve, the Outlet Purge Valve (OPV), located along the anodic exhaust line.

The purge process has been analyzed at different FC power output levels. For each FC power level the optimized behavior of the FC operation was found, by regulating the time of flooding.

The aim of this analysis is to optimize the purge process to reduce the amount of hydrogen discharged with water, in order to increase the FC efficiency. An investigation on the benefits in terms of fuel utilization factor and costs, resulting from optimization of the FC purge process, is shown in the paper.

1. Introduction

Hydrogen and Fuel Cell (FC) technologies offer a pathway to enable the use of clean energy systems to reduce emissions, improve energy efficiency and stimulate the global economy [1,2]. Many studies on conventional combustion-based energy system show that improvements could be still achieved on the efficiency side, but with enormous efforts in terms of plant complexity (see for example a couple of our studies [3–7]) and still with CO_2 and other pollutants production. FCs have several benefits over conventional combustion-based technologies currently used in many power plants. Greenhouse gases and air pollutants responsible of smog and health problems are avoided at the point of operation of FC systems. On a life-cycle basis, if pure H_2 is used as a fuel, FCs emit only heat and water as byproducts [2].

Among FC technologies, Proton Exchange Membrane (PEM) FCs gained increasing attention especially for the large characteristic power density, low operating temperature but still with CHP potential (for example for residential applications [8,9]), and safe operation. Significant effort is being made towards producing PEM systems able to achieve the optimum balance of cost, efficiency, reliability and durability.

The short lifetime of PEM-FCs is a barrier to the deployment and commercialization of this power generation system. FC lifetime requirements vary significantly, ranging from 3000

* Corresponding author. Tel.: +39 051 2093318; fax: +39 051 2093313.
E-mail address: andrea.depascale@unibo.it (A. De Pascale).

0360-3199/$ – see front matter
http://dx.doi.org/10.1016/j.ijhydene.2012.09.147

to 5000 operating hours for car applications, up to 40,000 operating hours for stationary applications [10–12]. Quantify the long-term performance and durability of an FC is currently still difficult. Indeed, all the mechanisms of FC components deterioration, affecting FC performance degradation, are not yet fully understood. The rate of degradation of the stack voltage is taken as a parameter indicative of the health status of an FC. Generally the range of voltage reduction rate is of 1–20 [μV/h] [11,12].

A phenomenon which particularly affects the longevity of a PEM-FC is the quality of water management. Inadequate water content, either globally within the stack or locally at certain locations within the unit cell, results in reduced conductivity in the membrane [13] and in any ions present in the catalyst layer. This results in increased ohmic losses and in a drop in cell voltage [10,12]. A balance must be realized between reactants (hydrogen and oxygen) delivery and water supply and removal [14]. St-Pierre et al. [15] showed that the life and longevity of an FC is strongly affected by the quality of water management in the PEM-FC. The management of water is critical for optimizing performance of a PEM-FC stack. In fact proper management of water within the cell ensures high efficiency, maintaining power density and stable operating conditions in the face of long periods of operation [16]. To this aim, it is necessary, on one hand, to keep the membrane humidified to have a high proton conductivity which is proportional to water content. On the other hand, an excessive accumulation of water (flooding) may negatively impact on the performance and lifetime of fuel cell.

In this paper an investigation on the flooding phenomenon of a commercial PEM-FC is carried out and a modification on the internal water management is implemented. The effects on FC performance are also analyzed. The investigation is based on the application and development of an experimental test bench.

2. The experimental test bench

The experimental test bench consists in a microgrid connecting several power sources and comprising in particular an FC system, designed to operate in island mode, but also connected to the external electric network (Fig. 1). The microgrid has been developed at the laboratory of the University of Bologna, as described more in detail in previous works by the authors [17–20]. Basically, this integrated energy system accommodates the following components:

- a PEM-FC stack, connected to a dedicated inverter;
- an electrochemical energy storage system (batteries) with a bidirectional inverter;
- a connection to external power sources;
- a load emulator subsystem;
- an electric board connecting the power sources inverters to the load emulator.

Fig. 1 shows the schematics of the electric microgrid where, in each branch, measuring sensors (indicated with S) and switch contactors allowing the opening or closing of branches, are installed.

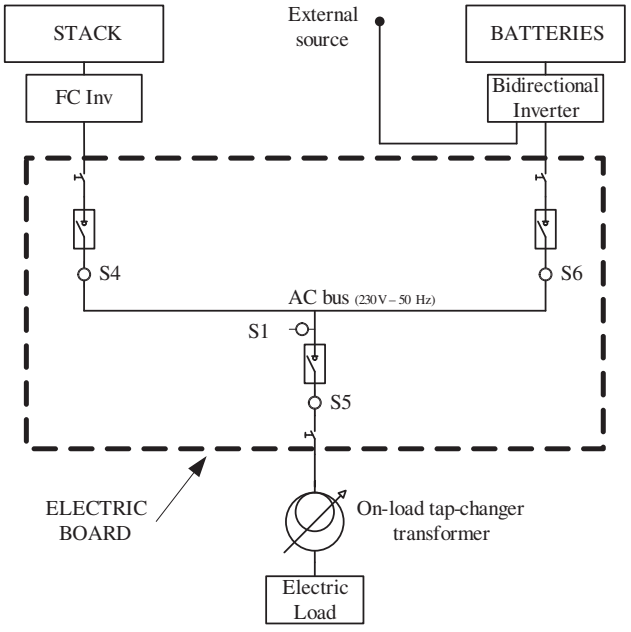

Fig. 1 – Experimental test bench.

The FC analyzed (Fig. 2), is a commercial H_2 fueled PEM-FC, rated for 4.5 kW of electric AC power, designed to operate at low temperatures (nearly 60 °C) at full load. The FC stack (Fig. 2b) is capable to provide 1–5 kW in DC, at voltage in the range 50–68 V and current intensity variable in the range 10–118 A [19].

In particular, Fig. 3 presents: (i) the supply circuits of fuel (in red); (ii) the air line (in light blue); (iii) the FC cooling system (in dark blue); and (iv) the stack and electric auxiliaries (in black). The FC cooling system comprises a tank of demineralized water, a pump (P), a heat exchanger (HX), where heat is transferred to an external CHP utilization circuit. In order to start-up the FC, a by-pass of the tank and a deviating valve DV is also positioned in the cooling circuit.

In the H_2 line, at the anode outlet side, the Outlet Purge Valve (OPV) is used, a valve operating in dead-end mode, i.e. accomplishing a periodic purging of the water (FC reaction product migrating in the anode compartment) and of the accumulating impurities.

The test bench is also endowed with a data acquisition system and the used sensors for current, voltage, temperature and mass flow rate are listed in Table 1. A real-time microcontroller, namely a National Instrument CompactRIO™ system [20,21], is used to acquire signals from sensors and to control the main input variables of the FC system and of the test bench (FC power set point, circuit breakers status). In order to simulate the external loads of different kind of users, a dedicated National Instrument control board is employed to generate different load scenarios.

3. The flooding phenomenon

Flooding is the accumulation of excess water which can occur at both the cathode and the anode side of the membrane [12].

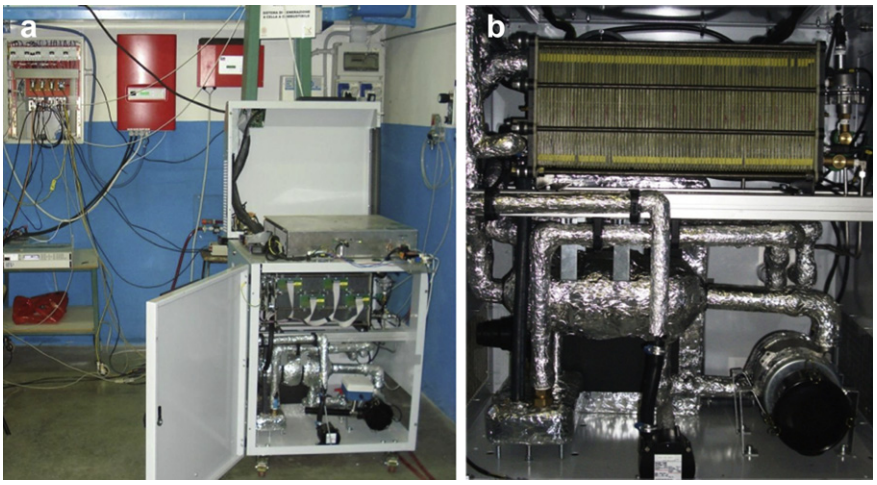

Fig. 2 – View of the FC system (a) and components (b).

The FC stack rated performance in terms of output DC current and voltage can be significantly diminished by the electrodes flooding phenomenon. The flooding phenomenon, whether it occurs in both electrodes or only in one, leads to a sudden increase of concentration losses (Fig. 4). Indeed, water blocks the pores of the gas diffusion layers and it prevents the reagents to reach the catalysts, causing a sudden voltage drop [11]. An excess of water promotes the corrosion of the electrodes, of the catalyst layers, of the bipolar plates and of the membrane [22]. Then, the impurities can be deposited on the catalysts. Hence, dissolved catalyst particles and the impurities can also be transported in the membrane replacing H+ ions. Consequently, ohmic losses increase, the electrodes performances decrease and the conductivity is reduced over the time, leading to FC failure [11,15].

Although the flooding at the anode occurs less frequently than the cathode [12,23], it is the most hazardous for the correct functionality of the cell. In fact it is able to cause the failure of the fuel necessary for the realization of electrochemical reactions and causes corrosion of the catalyst layer.

The flooding at the anode side is favored by:

- low hydrogen flow rates and by low current densities (0.2 A/cm^2), while high current densities will generates most intense electro-osmotic forces able to reduce the amount of water at the anode [22];

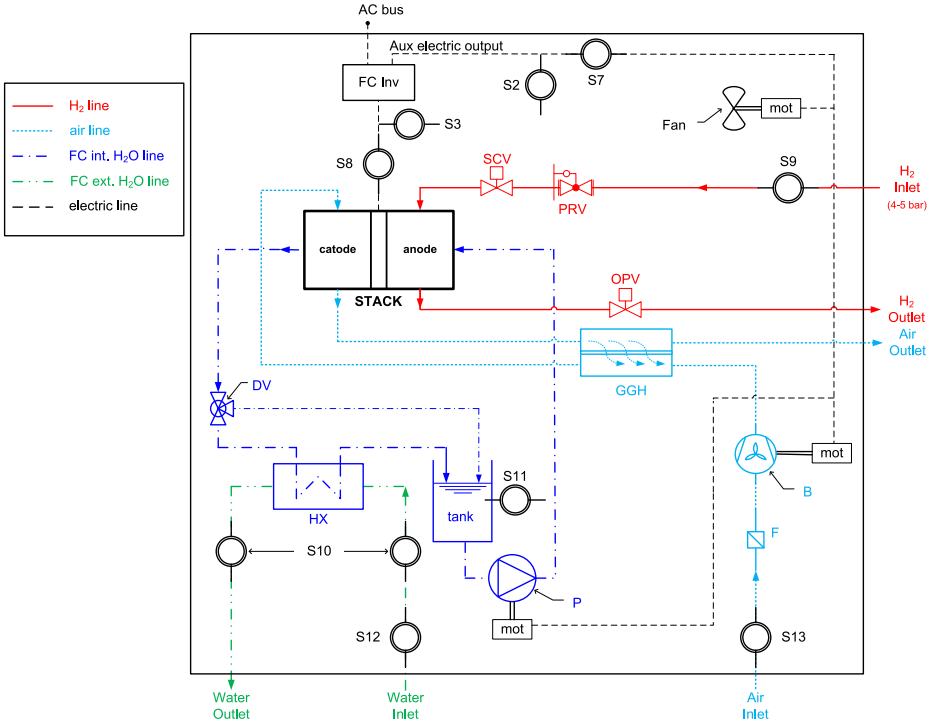

Fig. 3 – The FC system layout.

Table 1 – Measuring sensors.

Sensor	Type	Accuracy
S1, S2, S3	LEM LV25-P voltage transducers	±1.6% of reading (rdg)
S4, S5, S6, S7	LEM LA100-P current transducers	±0.45% of rdg
S8	LEM LA200-P current transducer	±0.40% of full scale
S9	Bronkhorst thermal H_2 flow meter	±0.8% of rdg plus ±0.2% of full scale
S10	K-series thermocouple	±1 °C
S11	J-series thermocouple	±1 °C
S12	McMillan Turbine water flow sensor	±0.50% of rdg
S13	GL gx Turbine air flow meter	±0.5% (linearity)

- lower cell temperatures and then by higher water condensation in the anode channels. Ge et al. [24] confirm that at the anode inlet, the proton flux is high and a strong electro-osmotic force drags the water molecules from the anode to the cathode, resulting in low water content. At the anode outlet, the current density is lower, hence the water content is higher;
- liquid water injected for cooling and humidification with conditions of low temperatures [24];
- water back-diffusion phenomenon, i.e. the diffusion of water from cathode to anode promoted by a low hydration state of the fuel gas stream [24,25].

Even in the absence of impurities, the prolonged exposure of the membrane-electrode assembly (MEA) to a high amount of water can cause a permanent FC performance loss linked to the degradation of materials.

To remove excess water and impurities inside the FC, it is necessary to operate a periodic purging.

4. The purge process analysis

The purge process has a fundamental role on the stability of the power supplied by the FC. Mokmeli et al. [16] showed that the amount and the concentration of impurities in the FC increases with time in absence of purge. Due to this increasing accumulation of impurities, the stack is characterized by loss of voltage increasing over time (Fig. 4).

For this reason the purge process should be periodically run in an FC energy system. To operate the purging, the OPV valve was installed downstream of the FC stack in study (Fig. 3). The purge occurs during the entire OPV opening time window. During this time, in addition to impurities, excess water and inert gas, also a quantity of fuel is discharged and thus it is not used by the FC electrochemical reactions. The amount of unreacted fuel varies with the amount of time between two consecutive purges, for given opening time of the OPV.

The two main control parameters of the periodic purge process and of the OPV installed in the FC object of the present study and investigated also in [16], are (as shown qualitatively by Fig. 5): i) the time between two consecutive purges, named here T_{fl}; and ii) the purge time, T_{pu}. T_{fl} is equal to the time interval in which the OPV is closed and thus water accumulates in the FC anodic side, causing flooding. T_{pu} is the time during which the OPV is open and thus impurities, inert gases and excess water are eliminated out of the FC.

The purge process setting typically consists in programming these two parameters as function of the FC voltage or as function of time [26]. The first approach called "purge controlled by the current" is based on the observation that the current varies when the FC accumulates both impurities and inert gases and the phenomenon of flooding starts. The sensors measure the current to detect this deviation and an electronic device activates the OPV opening.

The second purge programming approach instead is based on the setting of the OPV characteristic times, independently on the FC operating conditions in terms of current.

A simplified way to realize the purging process using the second approach consists in assuming constant values for both T_{pu} and T_{fl}. The values of these two parameters should be chosen as a tradeoff between the minimization of amount of discharged H_2 and of the voltage loss of the FC, resulting in an improvement in terms of fuel utilization.

Finally, the purge can be operated when the stack voltage equals a predetermined threshold value, with the aim to protect and preserve the longevity and performance of the FC.

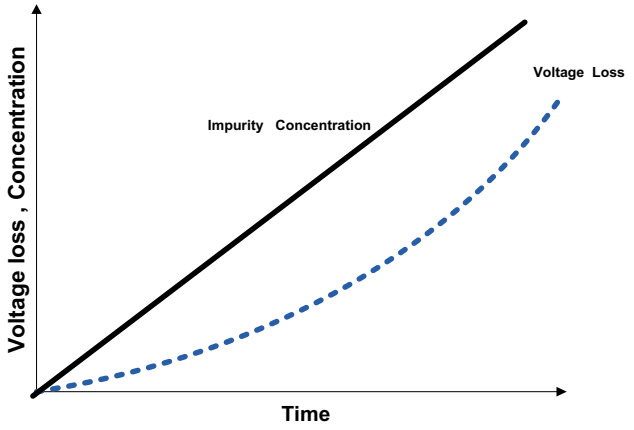

Fig. 4 – FC impurities concentration (continuous line) and FC stack voltage (dotted line) in absence of purge [9].

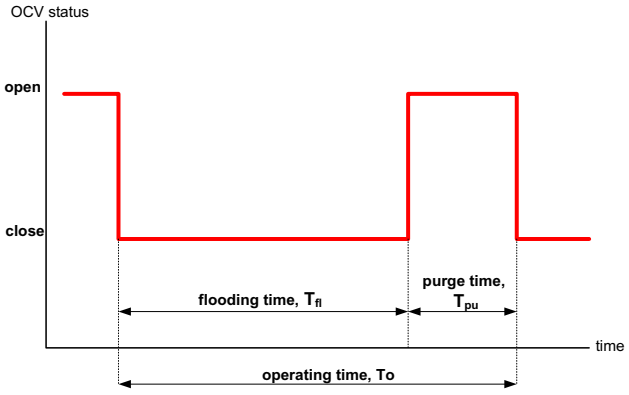

Fig. 5 – Characteristic time settings of purge process, according to [9].

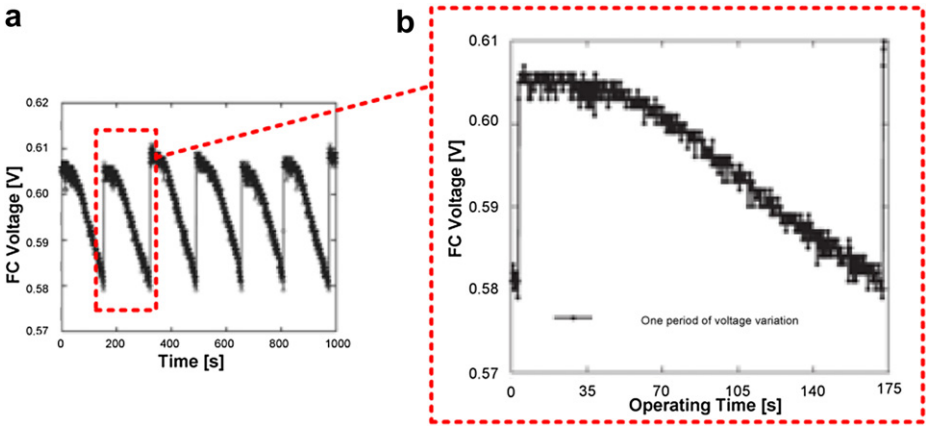

Fig. 6 – (a) FC stack voltage variation versus operating time; (b) one period of FC stack voltage variation.

The amount of purge time must be such as to allow recovery only of voltage loss. Fig. 6 shows the degradation of the FC stack voltage during the time when the OPV is closed (flooding time). This interval between two consecutive purges can be divided into two parts. In the first, the stack voltage is constant for a given value, which represents the absence of liquid water accumulation in the gas diffusion layers, then tension starts to decay. This effect is caused by the increasing water content in the FC, which compromises the correct occurrence of electrochemical reactions. In addition to the decay of the FC voltage, a fluctuation of H_2 pressure within the anode channels, linked to the dynamic process of purging, occurs. Pressure fluctuations might produce stress, mechanical vibrations and damages on MEA [16].

5. Experimental investigation on the effects of purge

An investigation on the flooding phenomenon and its effects on FC performance at different FC power output levels has been carried out. The aim of this analysis is to optimize the purging process, to increase FC lifetime (linked with the flooding occurrence) and to reduce the amount of H_2 discharged with water, in order to increase the fuel utilization factor and FC efficiency.

Different FC power levels have been investigated, by analyzing the FC performance depending on the purge time, in order to find the corresponding optimum purge process time settings.

Fig. 7 and Fig. 8 show the experimental trend of the FC voltage (blue line) and the H_2 mass flow rate (red line) versus time, during the time of few consecutive purges (with constant values of $T_{pu} = 2.5$ s and $T_{fl} = 20$ s), for two different FC power values, equal to 500 W and 1500 W respectively. The periodic OPV opening occurrence clearly induces a sudden increase of H_2 mass flow, measured at the FC anode inlet stream, which is not integrally absorbed by the electrochemical reactions. Indeed, the shown experimental trend of voltage undergoes a sudden drop when the OPV opening occurs. The plots of Figs. 7 and 8 also show the decrease of voltage due to flooding in the time period T_{fl} in which the OPV is closed.

Fig. 9 shows a simplified model of the voltage trend versus time during a single purge. In particular, in the flooding phase, when the OPV is closed, the FC voltage decreases and a linear mean trend versus time can be considered. At the opening of the OPV, i.e. at the beginning of the purge time, the stack voltage undergoes a sharp drop; the voltage trend versus time can be linearized also in this period. This behavior is related to the occurrence of a pressure drop of the H_2 stream within the stack (approximately decreasing from the value of 1.4 bar

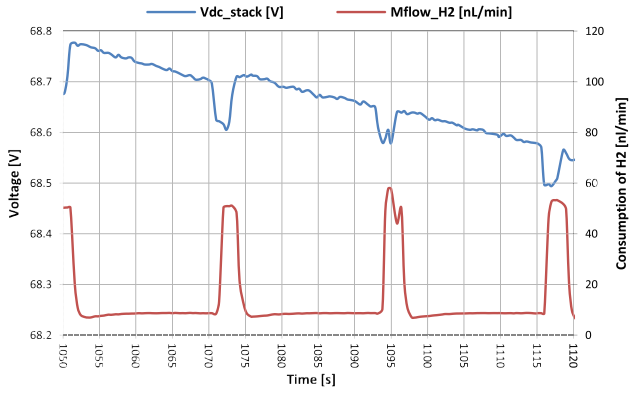

Fig. 7 – FC voltage and H_2 mass flow trend vs time, when $P_{FC} = 500$ [W], ($T_{pu} = 2.5$ s and $T_{fl} = 20$ s).

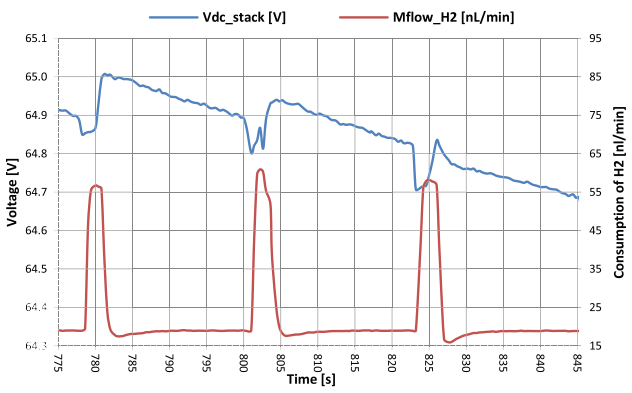

Fig. 8 – FC voltage and H_2 mass flow trend vs time, when $P_{FC} = 1500$ [W], ($T_{pu} = 2.5$ s and $T_{fl} = 20$ s).

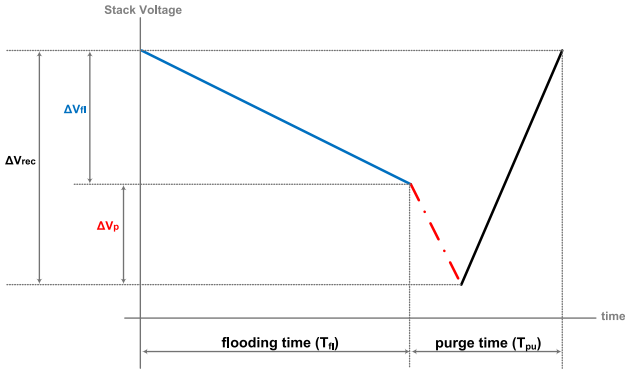

Fig. 9 – Linearized trend of voltage during a purge period; the flooding phase (ΔV_{fl}, in blue), the pressure drop phase (ΔV_p, in red) and the recovery phase (ΔV_{rec} in black). (For interpretation of the references to color in this figure legend, the reader is referred to the web version of this article.)

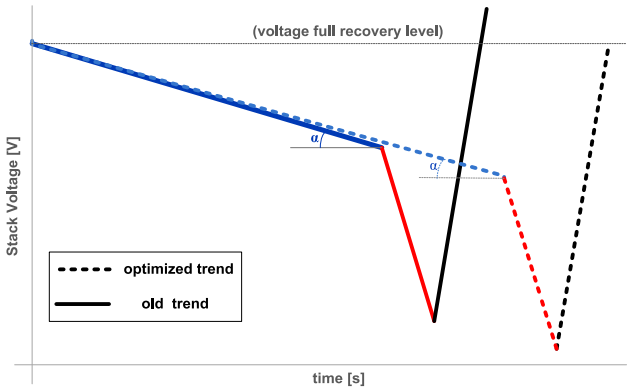

Fig. 10 – Original (continuous lines) and optimized (dotted lines) stack voltage trend during the flooding time and the purge time, for a constant FC power output value.

down to 1 bar). Thus, the purge time period can be divided into the pressure drop phase and the recovery phase, respectively. Each of all these phases are here modeled with a linear trend, as shown in Fig. 9.

According to the study reported in [26], the purge process is optimized when the amount of voltage recovered at the time of OPV opening equals the voltage drop occurring between two consecutive purges. The optimization of purge settings can be described by the following equation:

$$\Delta V_{fl} + \Delta V_p = \Delta V_{rec} \quad (1)$$

where, as show in Fig. 9, ΔV_{fl} is the FC voltage drop during the flooding; ΔV_p is the sudden FC voltage drop related to the phenomenon of the OPV opening; ΔV_{rec} is the voltage recovered after the OPV opening, due to the elimination of the internally accumulated water.

The above described model has been used to optimize the purge process depending on the FC power output set point. Five different operating points have been analyzed, with a FC power output level equal respectively to: 500 W; 1500 W; 2500 W; 3500 W; 4500 W.

The original OPV control strategy provided by the FC manufacturer was a simple logic in which the OPV opening time T_{pu} and the T_{fl} time where kept constant independently on the FC power output. For each investigated FC power level, the corresponding optimum purge settings have been analyzed. For each point, the optimized behavior of the FC has been found extending or reducing the T_{fl}, i.e. the time during which the OPV is closed, while the T_{pu} time has been kept constant.

A comparison between the original FC stack voltage not optimized behavior with the optimized one, in the same period of purge, is carried out.

To obtain the optimized FC voltage behavior, for each of the five selected power set points, eq. (1) has been applied considering the quantities ΔV_p and ΔV_{rec} constant and ΔV_{fl} variable. Eq. (1) can be rewritten as:

$$\alpha T_{fl} + \Delta V_p = \Delta V_{rec} \quad (2)$$

where α is the slope of the straight line modeling the FC voltage behavior during the flooding; T_{fl} is the flooding phase time, i.e. the time between two consecutive purges.

Fig. 10 shows, for a single purge, the comparison between the actual behavior (continuous lines) of the FC stack voltage, estimated by linear trends with the above described model, and the "optimized" behavior (dotted lines), obtained applying eq. (2). In particular, the blue lines indicate the voltage drop during the flooding; the red ones indicate the voltage drop due to the pressure drop at the OPV opening and the black lines indicate the voltage recovery.

6. Analysis of the FC purge programming logic

The purge process programming logic currently implemented in the PEM-FC is a function of time.

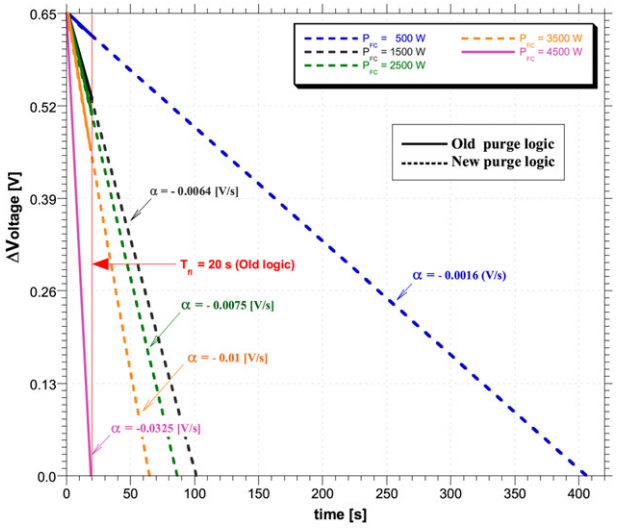

Fig. 11 – FC voltage drop vs time adopting current purge process settings (continuous lines) and new logic (dashed lines), for different FC power set points.

Table 2 – The flooding time (T_{fl}) versus FC power, old and new optimized purge process settings.

FC power P_{FC} [W]	Old purge T_{fl} [s]	Optimized purge T_{fl}^{+} [s]
500	20	406.2
1500	20	101.5
2500	20	86.6
3500	20	65
4500	20	20

In particular, the original values of T_{fl} and T_{pu} were set by the manufacturer and are respectively equal to 20 s and 2.5 s, both kept constant for each FC power output set point. This purge process time setting is optimized for the maximum FC power (4.5 kW), but it is very inefficient for low and medium FC power. This is due to considerable unreacted H_2 loss during the opening time of the OPV.

To reduce the amount of unreacted and expelled H_2 during the purge and at the same time safeguarding the FC internal components, it is necessary to improve the implemented purge logic, by optimizing the purge process time settings.

The aim of this purge process optimization is to increase the fuel utilization factor, U_f, defined as the ratio between the theoretical fuel chemical energy ($\dot{m}_M$), necessary to bring about the electrochemical reactions, and the introduced fuel chemical energy ($\dot{m}_{H_2}$):

$$U_f = \frac{\dot{m}_M}{\dot{m}_{H_2}} \tag{3}$$

The increase of U_f leads also to an increase of the FC efficiency, η which is directly linked to U_f.

To optimize the purge process a new purge time programming logic has been adopted to investigate the flooding time effect. In this new logic the values of purge parameters differ according to the FC power output. In particular, the T_{fl} of the five operating points, at different FC power levels, is studied imposing a maximum permissible FC voltage drop during flooding, ΔV_{max}, and keeping the T_{pu} value constant, equal to 2.5 s. The ΔV_{max} value has been fixed equal to the actual FC voltage drop during the flooding phase at FC maximum power (equal to 0.65 V).

The calculation of the optimum T_{fl} using the new purge logic is performed using a linear trend model of the FC voltage drop versus time, as introduced in the previous paragraph. Thus, according to eq. (2), for each of the five FC power levels, the optimized T_{fl} value has been obtained by solving the simple equation:

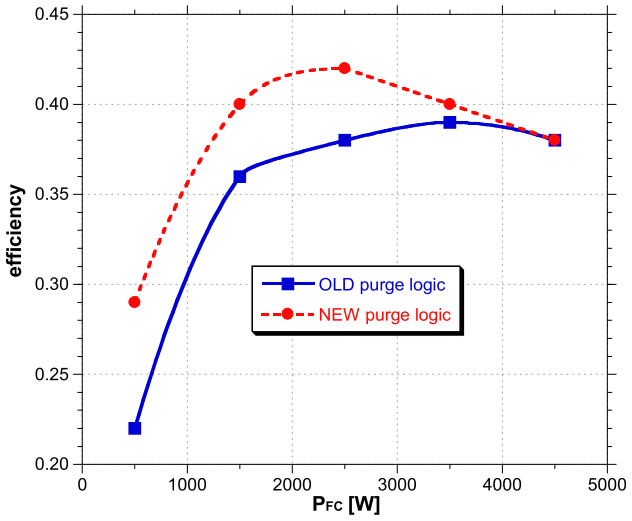

Fig. 12 – FC efficiency versus FC output power in the original purge programming logic (continuous line) and in the optimized one (dotted line).

$$\alpha T_{fl} + \Delta V_{max} = 0 \tag{4}$$

Fig. 11 shows the FC voltage drop behavior versus time: the value of α varies with the FC power set point; thus, using the original purge logic (continuous lines in Fig. 11) with fixed T_{fl} the final voltage drop at the end of the flooding time is completely different depending on the FC set point.

By using the new purge programming logic (dashed lines) the OPV time setting can be modulated depending on the FC power set point. For a given FC power output set point, the optimized T_{fl} can be read on the x-axis, where the ΔV value (along the dotted lines) reduces to zero. The optimal flooding time value obtained by purge process time setting management is shown in Table 2.

The mean values for the input power (P_M) with reference to the fuel LHV, for the H_2 mass flow rate (m_{H_2}) and for the FC efficiency (η) have been calculated by time-averaging the instantaneous values over a time window τ, in which the FC set point was kept constant. This time period τ was chosen sufficiently long to include a high number of purges. Table 3 shows the values of P_M, m_{H_2} and η obtained using the original purge programming logic and the new one (values with the superscript $^{+}$), for each of the five FC power set points, respectively.

FC efficiency versus mean fuel inlet power, shown in Fig. 12, increases using the optimization of the purge process (dotted

Table 3 – Mean fuel input power, H_2 mass flow rate, FC efficiency and energy saving with the new purge logic.

FC power setting	Old purge logic			New purge logic			ΔE [–]
P_{FC} [W]	P_M [W]	m_{H_2} [kg/s]·10^5	η [–]	P_M^{+} [W]	$m_{H_2}^{+}$ [kg/s]·10^5	η^{+} [–]	
500	2273	1.89	0.22	2942	2.45	0.29	30.0
1500	4167	3.47	0.36	4688	3.91	0.40	12.9
2500	6579	5.48	0.38	7576	6.31	0.42	7.6
3500	8975	7.48	0.39	9210	7.67	0.40	2.9
4500	11840	9.87	0.38	11840	9.87	0.38	0.0

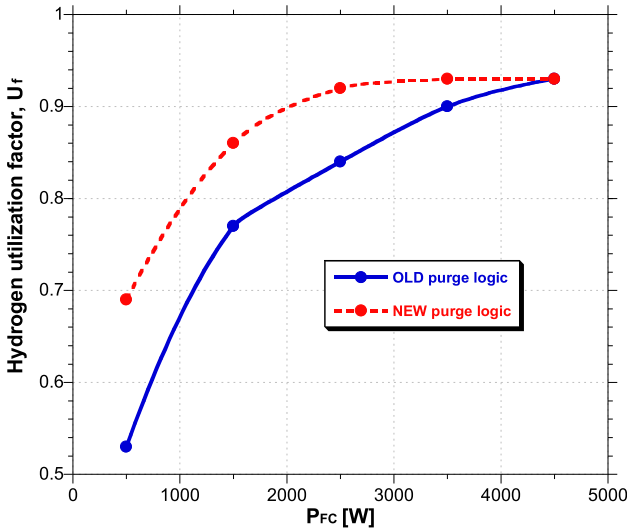

Fig. 13 – The fuel utilization factor using original purge programming logic (U_f) and the new one (U_f^+).

red line). In particular, this benefit occurs at low and medium FC power, (Fig. 12), where the actual purge logic provided lower performance. This variation in efficiency, could be explained considering the improvement in fuel saving achieved by reducing the purge valve opening frequency. The savings of fuel input energy introduced into the FC, obtained using the new purge programming logic, is also shown in Table 3; it has been evaluated using the following expression:

$$\Delta E = 1 - \left[\frac{E^+}{E}\right] \tag{5}$$

where:

$$E = \int_0^\tau m_{H_2} \cdot LHV \cdot dt \tag{6}$$

$$E^+ = \int_0^\tau m_{H_2}^+ \cdot LHV \cdot dt \tag{7}$$

E and E^+ are the mean fuel input energy introduced into the FC during the time τ, evaluated respectively in the old and new purge logic.

Fig. 13 shows the change of the H_2 utilization factor according to maximum percentage saving, using both the old purge logic (U_f) and the new one (U_f^+). Further improvements in fuel utilization factor (even if its maximum could be in principle equal to 100%) seem difficult to achieve by modifying further the purge logic at part load conditions (in the range 1500–3500 W), as the shown new obtained values in this range are close to the value at full load.

7. Conclusions

In this paper an investigation on the flooding phenomenon of a PEM-FC, with effects in terms of performance degradation, has been performed. In particular, the analysis was focused on the purge process at the anode side of the PEM and the purge operation that allows to recover the instantaneous FC voltage drop has been investigated.

The purge process has been examined in five different FC power set points. To overcome the inefficiency of the actual purge programming logic implemented in the PEM-FC at low and medium FC power output, the optimization of the OPV valve characteristic times has been carried out. A new purge programming logic, characterized by variable flooding time and constant purge time has been tested. Using this new logic the FC efficiency increases significantly, especially at part-load, obtaining a saving in terms of input fuel energy.

Finally, it has been shown that the optimized purge process allows to increase the fuel utilization factor. To further increase the fuel utilization factor at minimum FC power output, a change in the anodic side outlet circuit of the FC, could be realized. In particular, a recirculating circuit of unreacted H_2 (expelled during the purge time) could be created downstream the OPV. This feature, not investigated in this study, could be considered in future developments.

Nomenclature

Symbols

E	fuel input energy with reference to LHV, [kJ]
m	hydrogen mass flow rate, [kg/s]
P_{FC}	FC power level, [W]
T_{fl}	flooding time, [s]
T_o	operating time, [s]
T_{pu}	purge time, [s]
U_f	fuel utilization factor, [-]

Greeks

α	slope of the straight line of the FC voltage, [V/s]
η	efficiency, [–]
ΔE	fuel chemical energy introduced into the FC, [kJ]
ΔV_{fl}	FC voltage drop during the flooding time, [V]
ΔV_{max}	maximum allowable FC voltage loss, [V]
ΔV_p	FC voltage drop during the purge time, [V]
ΔV_{rec}	FC voltage recovery after the OPV opening, [V]
τ	time with FC at constant power, [s]

Acronyms and subscripts

AC	Alternate Current
CHP	Combined Heat and Power
DC	Direct Current
DV	Directional Valve
FC	Fuel Cell
GGH	Gas–Gas Humidifier
H_2	Hydrogen
HX	Heat exchanger
LHV	Low Heating Value
MEA	Membrane-Electrode Assembly
OPV	Outlet Purge Valve
P	Pump
PEM	Proton Exchange Membrane
PRV	Pressure Reducing Valve

rec	recovery
S	measuring Sensors
SCV	Safety Control Valve

REFERENCES

[1] European Commission. EUR 20719 EN – hydrogen energy and fuel cells – a vision of our future, http://ec.europa.eu/research/energy/; 2003.

[2] Fuel cell handbook. 7th ed. US: DOE; 2004.

[3] Bhargava RK, Bianchi M, Campanari S, De Pascale A, Negri di Montenegro G, Peretto A. A parametric thermodynamic evaluation of high performance gas turbine based power cycles. Transaction of the ASME. Journal of Engineering for Gas Turbines and Power 2010;132. p. 022001–1/14.

[4] Bianchi M, Branchini M, De Pascale A, Melino F, Peretto A, Bhargava RK, et al. Gas turbine power augmentation technologies: a systematic comparative evaluation approach. Proceedings of ASME Turbo Expo 2010, [vol.] 5, art. no. GT2010-22948, p. 99–107.

[5] Bagnoli M, Bianchi M, Melino F, Peretto A, Spina PR, Bhargava R, et al. Application of a computational code to simulate interstage injection effects on Ge frame 7ea gas turbine. Transaction of the ASME. Journal of Engineering for Gas Turbines and Power 2007;130(Issue 1). p. 012001–1/10.

[6] Bianchi M, Melino F, Peretto A, Spina, PR, Ingistov S. Influence of water droplets size and temperature on wet compression. Proceedings of ASME Turbo Expo 2007, May 14–17, 2007, Montreal, Canada, [vol.] 3, p. 651–62.

[7] De Pascale A, Ferrari C, Melino F, Morini M, Pinelli M. Integration between a thermo-photo-voltaic generator and an organic rankine cycle. Applied Energy September 2012;97: 695–703, http://dx.doi.org/10.1016/j.apenergy.2011.12.043.

[8] Bianchi M, De Pascale A, Spina PR. Guidelines for residential micro-CHP systems design. Applied Energy 2010;88(5): 1500–9.

[9] Bagnoli M, De Pascale A. Performance evaluation of a small size cogenerative system based on a PEM fuel cell stack. Proceedings of the ASME Turbo Expo 2005, [vol.] 4, art. no. GT2005-68451, p. 143–50.

[10] Knights SD, Colbow KM, St-Pierre J, Wilkinson DP. Aging mechanisms and lifetime of PEFC and DMFC. Journal of Power Sources 2004;127:127–34.

[11] Schmittinger W, Vahidi A. A review of the main parameters, influencing long-term performance and durability of PEM fuel cell. Journal of Power Sources 2008;180:1–14.

[12] Hinds G. Performance and durability of PEM fuel cells: a review. NPL report DEPC-MPE 002, 2004, p. 25–42.

[13] Zawodzinski T, Derouin C, Radzinski S, Sherman R, Smith V, Springer T, et al. Water uptake by and transport through nation 117 membranes. Journal of Electrochemical Society 1993;140(4):1041–7.

[14] McKay DA, Siegel JB, Ott W, Stefanopoulou AG. Parameterization and prediction of temporal fuel cell voltage behavior during flooding and drying conditions. Journal of Power Sources 15 March 2008;178(1):207–22.

[15] St-Pierre J, Wilkinson DP, Knights S, Bos M. Relationship between water management, contamination and lifetime degradation in PEFC. Journal of New Materials for Electrochemical Systems 2000;3:99–106.

[16] Mokmeli A, Asghari S. An investigation into the effect of anode purging on the fuel cell performance. International Journal of Hydrogen Energy 2010;35:9276–82.

[17] Bagnoli M, Belvedere B, Bianchi M, Borghetti A, De Pascale A, Paolone M. A feasibility study of an auxiliary power unit based on a PEM fuel cell for on-board applications. Journal of Fuel Cell Science and Technology 2006;3(4):445–51.

[18] Belvedere B, Bianchi M, De Pascale A. Experimental analysis of a cogenerative performance of a PEM fuel cell based energy system, Proceedings of ICAE 2011, 16–18 May 2011, Perugia, Italy.

[19] Belvedere B, Bianchi M, Borghetti A, De Pascale A, Di Silvestro M, Paolone M. DSP-controlled test set-up for the performance assessment of an autonomous power unit equipped with a PEM fuel cell. Proceedings of the 2007 international conference on clean electrical power (ICCEP'07), art. No. 4272427, p. 468–73.

[20] Belvedere B, Bianchi M, Borghetti A, Paolone M. Design, implementation and testing of an automatic power management system for residential stand-alone microgrid with power supply. Preprints of the 18th IFAC world congress, August 28–September 2, 2011, Milano (Italy).

[21] CompactRIO™ reference and procedures help (FPGA interface). National Instruments Corporation, http://www.ni.com/dataacquisition/compactrio/; 2004–2010.

[22] McKay DA, Ott WT. Stefanopoulou AG. Modeling, parameter identification, and validation of reactant water dynamics for a fuel cell stack. Proceeding of the IMECE, ASME international mechanical engineering congress exposition, 2005.

[23] Choi JW, Hwang YS, Cha SW, Kim MS. Experimental study on enhancing the fuel efficiency of an anodic dead-end mode electrolyte membrane fuel cell by oscillating the hydrogen. International Journal of Hydrogen Energy 2010;35:12469–79.

[24] Ge S, Wang CY. Liquid water formation and transport in the PEFC anode. Journal of Electrochemical Society 2007;154(10): B998–1005.

[25] Nguyen TV, White RE, Water A, Management Heat. Model for proton-exchange-membrane fuel cells. Journal of Electrochemical Society 1993;140:2178–86.

[26] Gou J, Pei P, Wang Y. The dynamic behaviour of pressure during purge process on the anode of a PEM fuel cell. J Power Sources 2006;162:1104–14.